Pacific Northwest
NATIONAL LABORATORY

PNNL-ACT-10127

Avista CEF2
Shared Energy Economy

Modeling and Simulation

October 31, 2022

TE McDermott J Xie M Ramesh

U.S. DEPARTMENT OF ENERGY

Prepared for the U.S. Department of Energy
Under contract DE-AC05-76RL01830

DISCLAIMER

PACIFIC NORTHWEST NATIONAL LABORATORY
operated by
BATTELLE
for the
UNITED STATES DEPARTMENT OF ENERGY
under Contract DE-AC05-76RL01830

Printed in the United States of America

Available to DOE and DOE contractors from the Office of Scientific and Technical Information,
P.O. Box 62, Oak Ridge, TN 37831-0062
www.osti.gov
ph: (865) 576-8401
fax: (865) 576-5728
email: reports@osti.gov

Available to the public from the National Technical Information Service
5301 Shawnee Rd., Alexandria, VA 22312
ph: (800) 553-NTIS (6847)
or (703) 605-6000
email: info@ntis.gov
Online ordering: http://www.ntis.gov

PNNL-ACT-10127

Avista CEF2
Shared Energy Economy

Modeling and Simulation

October 31, 2022

TE McDermott J Xie
M Ramesh

Prepared for
the U.S. Department of Energy
Under Contract DE-AC05-76RL01830

Pacific Northwest National Laboratory
Richland, Washington 99354

Abstract

This research project supported Avista's Shared Energy Economy (SEE) Project in Spokane's University District (UDistrict), as funded by the WA Department of Commerce Clean Energy Fund (CEF) Phase 2. The SEE project comprises a microgrid with two campus buildings, two solar photovoltaic generators, and two batteries. The microgrid can operate grid-connected or off-grid. This research project included modeling the buildings and other microgrid components, simulating a transactive energy system, and supporting Avista's testing of different use cases for the WA Department of Commerce. The main research finding is that buildings can be modeled successfully in a data-driven approach.

Acronyms and Abbreviations

3HT12F1	feeder designator for backup supply to SEE
3HT12F7	feeder designator for normal supply to SEE
A	current (Amperes)
ACT	agreement to commercialize technology
ASHRAE	American Society of Heating, Refrigerating and Air-Conditioning Engineers
ATS	automated transfer switch
BESS	battery energy storage system
BSET	battery system evaluation tool
CAP	capacitor bank on the feeder layout map
CCRS	Center for Clinical Research and Simulation
CEF	Clean Energy Fund
CIM	Common Information Model, referenced in IEC Standard 61970
Δ	change in a quantity
d	per-unit voltage change at the PCC
degF	degrees Fahrenheit
DER	distributed energy resources
DMS	distribution management system
DOC	Washington Department of Commerce
DOE	U.S. Department of Energy
dP	change in real power
dQ	change in reactive power
DSC	disconnect switch on the feeder layout map
dT	change in temperature
EERE	Office of Energy Efficiency and Renewable Energy at DOE
EWU	Eastern Washington University
ft	feet
FUSE	fuse on the feeder layout map
G	total solar irradiance, direct plus diffuse
GridLAB-D	an open-source distribution system simulator
HELICS	Hierarchical Engine for Large-scale Infrastructure Co-simulation
HSB	Health Sciences Building
HSCI	Health Sciences building's rooftop PV
HVAC	heating, ventilating, and air conditioning system in a building
IBR	inverter-based resources
IEC	International Electrotechnical Commission
IEEE	Institute of Electrical and Electronics Engineers
I/O	input/output
JMP	jumper on the feeder layout map
k	coefficient of building temperature response to price, $/degF
kV	kilovolts

kVLL	kilovolts line-to-line, between phases
kW	kilowatts
ML	machine learning model
MVA	megavoltamperes
MW	megawatts
NOAA	National Oceanic and Atmospheric Administration
NODE	connection node on the feeder layout map
p	price in a market bid or clearing
P	active power or real power
PCC	point of common coupling
PF	power factor
PMU	phasor measurement unit
PNNL	Pacific Northwest National Laboratory
PV	solar photovoltaic generation
q	quantity in a market bid or clearing
Q	reactive power
Q_{avg}	average reactive power
R	resistance
RD&D	research, development, and deployment
REC	recloser on the feeder layout map
RTU	remote terminal unit
SCADA	supervisory control and data acquisition system
SCAMP	South Campus building's rooftop PV
SEE	Shared Energy Economy
SEL	Schweitzer Engineering Laboratories
SMA	a solar inverter vendor, "System, Mess and Anlagentechnik"
SoC	state of charge in a battery, per-unit of capacity
SRC	transmission source on the feeder layout map
SWT	load-break switch on the feeder layout map
T	temperature
TEACH	Spokane Teaching Health Clinic
TESP	transactive energy simulation platform
UNK	unknown component on the feeder layout map
V	voltage
V_{avg}	average voltage
VB	virtual battery
V_T	terminal voltage at the PCC
WA	State of Washington
W_{avg}	average real power
WSU	Washington State University
X	reactance
XFM	transformer on the feeder layout map
Z_{sc}	short-circuit impedance

Acknowledgments

The authors would like to acknowledge the funding support from Avista Corporation through Agreement to Commercialize Technology (ACT) contract 73647A.

The authors also thank Mike Diedesch, John Gibson, Ben Shannon, and Kenneth Wilhelm of Avista for valuable guidance during the project. Anjan Bose and Monish Mukherjee of Washington State University (WSU) Electrical Engineering Department collaborated on transactive experiment designs. William Pierce and Andrew Hersman of WSU Facilities Department provided information about the buildings, and arranged for load shedding tests. John Dolan of McKinstry Associates provided an eQUEST model and other information about the buildings. Sen Huang of PNNL converted the eQUEST models to EnergyPlus.

Contents

Figures

Tables

1.0 Introduction

This project supported Avista's Shared Energy Economy (SEE) Project in Spokane's University District, as funded by the WA Department of Commerce Clean Energy Fund Phase 2 (CEF2). The main focus was transactive energy simulation, modeling of campus buildings, and use case testing. A parallel project, funded from the U.S. Department of Energy (DOE), provided battery economic evaluations and analytics.

The SEE project includes two campus buildings with upgraded controls and rooftop photovoltaic (PV) generators rated 100 kW each, and two battery energy storage systems (BESS) rated 167.5 kW and 500 kW. The two campus buildings are the Center for Clinical Research and Simulation (CCRS), and the Health Sciences Building (HSB), both part of the Washington State University (WSU) campus in Spokane. Avista installed both rooftop PV generators by October 2018, and both BESS by July 2020. The initial building models were developed by August 2020 for EnergyPlus at PNNL. To support improved building models, Avista collected 3-second revenue meter data from the two campus buildings (Figure 1) from January 23, 2019 to December 19, 2020, supplemented with 5-second SCADA data from two local feeders (Figure 2). PNNL supported use case testing of the microgrid done by Avista and WSU in August 2021, and specified building load response tests by WSU from March 3-7, 2022. Supply chain issues and the Covid pandemic may have affected these time frames, but all planned activity was completed.

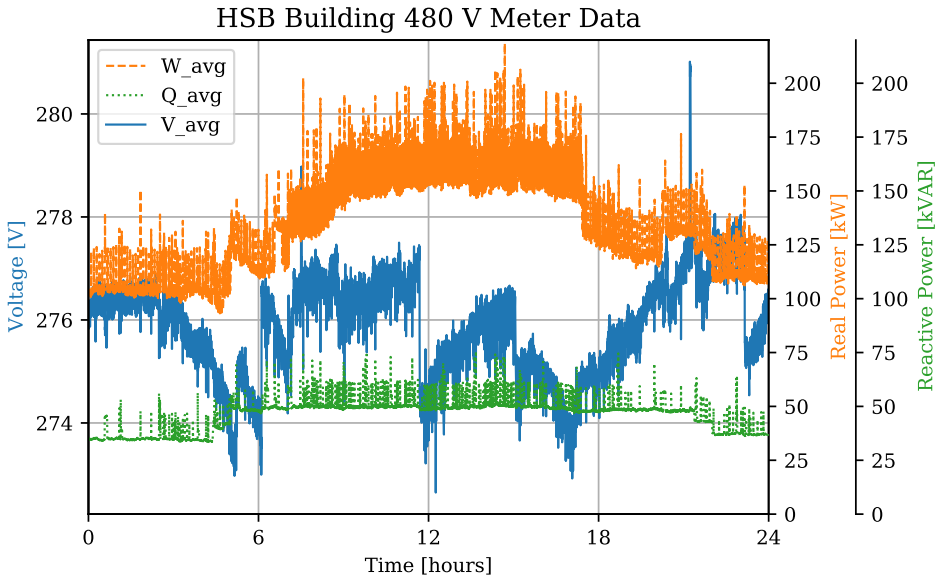

Figure 1. 3-second revenue meter data from HSB building.

The PNNL tasks included:

1. Coordinate and support WSU use of the Transactive Energy Simulation Platform (TESP), which integrates the GridLAB-D simulator [1] with separate software agents that implement transactive energy systems. TESP also generates output that is compatible with tool sets used for economic assessment in Task 4. Using TESP allows researchers to focus their effort on the new transactive methods, rather than building models and simulations. WSU

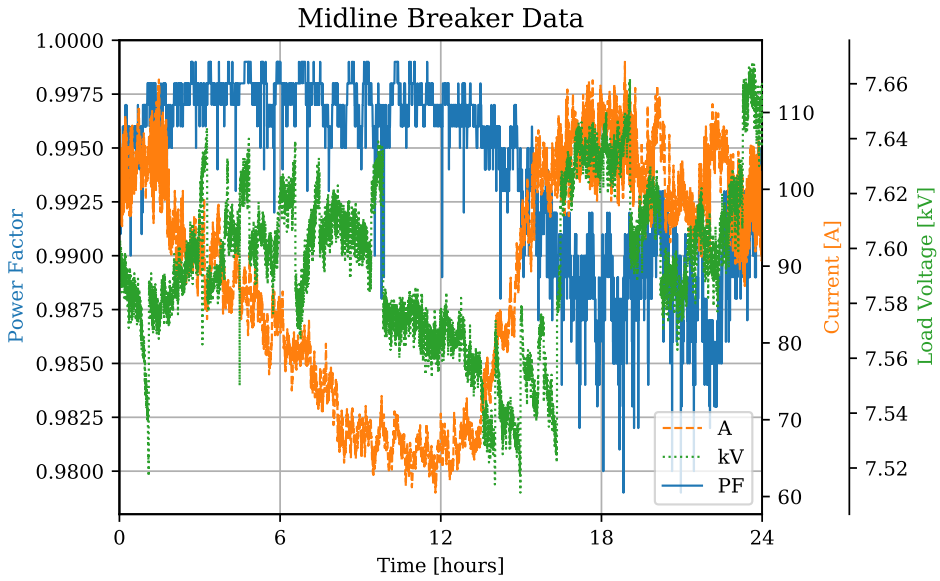

Figure 2. 5-second SCADA data from one of the feeders.

researchers were already using TESP for cybersecurity work. PNNL provided support in modeling the SEE, implementing transactive software agents, and running the simulations. WSU researchers designed transactive software agents and test plans for virtual experiments. WSU researchers and PNNL presented test plans to Avista and WSU Facilities for approval.

2. Develop and test a real-time battery controller agent that works in systems with multiple batteries. This agent did not use methods from the PNNL Battery System Evaluation Tool (BSET), which was designed to evaluate a single battery using defined data. The new agent manages multiple assets as virtual batteries (VB) in a consensus transactive energy mechanism, using data streams that emulate operation in real time. The VB agents are for experimental use, and not intended to replace the role of the Spirae company's dispatch system software for operations.

3. Characterize the dynamic behavior and transactive participation capabilities for the CCRS and HSB. This data is essential for designing transactive mechanisms that work properly, when there are no detailed building models available. A traditional building energy audit does not provide all the necessary information on load dynamics.

4. Provide technical support on smart inverter functions, IEEE 1547-2018, distribution platform standards, BESS acquisition, and grid modeling.

Avista proposed the CEF2 SEE project to illustrate four use cases. This project supported evaluation of each use case:

1. Grid Service: includes volt/var management, frequency response, capacity management, etc. PNNL used feeder models to estimate voltage response at the point of common coupling (PCC) to changes in DER real and reactive power. The transactive mechanism provided a means of managing feeder capacity.

2. Distributed Energy Resource (DER) Optimization: includes tariff optimization scenarios, transactive energy, etc. The consensus transactive mechanism allowed each DER to participate

in a hypothesized market, with an opportunity to optimize its economic outcome.

3. Building Fleet Optimization: includes campus demand reduction, coordination with DERs, etc. The improved building model allowed each building agent to participate more effectively in load dispatch schemes, whether by transactive energy or conventional demand response.

4. Critical Resiliency: includes islanded operation. PNNL used feeder models to estimate resource balance in the microgrid during off-grid operations. The transactive energy mechanism could provide an alternative method of balancing resources during off-grid operation.

Section 2.0 of this report describes the methods and results of modeling CCRS and HSB. Section 3.0 describes how the building models were used with a reduced-order feeder model to perform transactive energy simulations of the SEE project. Section 4.0 describes how the four main CEF2 SEE uses cases were tested, with PNNL support, after all resources and essential control systems had been installed. Section 5.0 summarizes the main findings and offers recommendations for future work.

2.0 Campus Building Model Development

An energy audit of the CCRS and HSB produced summary load information in Table 1, and a computer model of each building in eQUEST [2]. PNNL was then able to derive a model of each building in EnergyPlus [3], including default subsystems for heating, ventilating, and air conditioning (HVAC). To implement time-dependent load behavior in these EnergyPlus models, we added typical schedules of occupancy, and power densities (W/m^2) for lighting and plug loads. Table 1 provided some information on appropriate power densities for CCRS and HSB. Utility revenue meter data provided some data for overall calibration of the building load levels. During an EnergyPlus simulation, weather changes and people occupy the building, which affects the electrical demand. The EnergyPlus model represents total real power demand, at hourly intervals, through these changes.

Table 1. Energy Audit Information

Load Survey	CCRS [kW]		HSB [kW]	
Category	**Min**	**Max**	**Min**	**Max**
HVAC	9	73	113	296
Plug Loads	18	18	116	117
Lighting	80	143	185	188
Total	**107**	**234**	**414**	**601**

To test the EnergyPlus models, we ran them in a transactive energy simulation, using components that come with TESP [4]. There are two building models depicted in Figure 3, each of which responds to a thermostat settings change, ΔT. Software agents implemented in *eplu_agent_helics.cpp* and *consensus.cpp* bid their building's load responsiveness into the electricity market, based on a slope k that relates value to temperature change. In the consensus mechanism, each agent receives all other bids so that the cleared price, p, and quantity, q, can be determined locally. GridLAB-D simulates the electric utility feeder with its other loads. If the total feeder load, including both buildings, exceeds the capacity, Cap, the utility will submit a bid for load reduction. In this example, there can be up to three bids for each market clearing interval of 5 minutes. Each agent stores its own metrics for post-processing. HELICS, which is built into TESP, manages the time synchronization and messaging between the agents and simulation federates.

Figure 4 shows the GridLAB-D output from a simulation of two summer days in TESP. The base feeder load is about 1700 kW, plus the CCRS and HSB building loads. In this model, the EnergyPlus building loads are non-zero only during daylight hours. The two solar DER reach an aggregate peak of 200 kW on the second day, and somewhat less on the cloudy first day. The two batteries are on idle. The aggregate DER generation is included in the substation's total real power. The feeder model is simplified, but it does reproduce a voltage drop at the building meters under load. In this simulation, all of the meter bills increase steadily.

Figure 5 shows the CCRS EnergyPlus outputs from this two-day simulation. The left-hand column shows the volume average zonal thermostat setpoints and temperatures. The outdoor air temperature comes from weather data for the Spokane airport. The thermostat $Schedule$ setpoints are assumed building defaults. To emphasize the simulation features, a day-to-night difference of 15 degF has been programmed for the setpoints, i.e., larger than would be

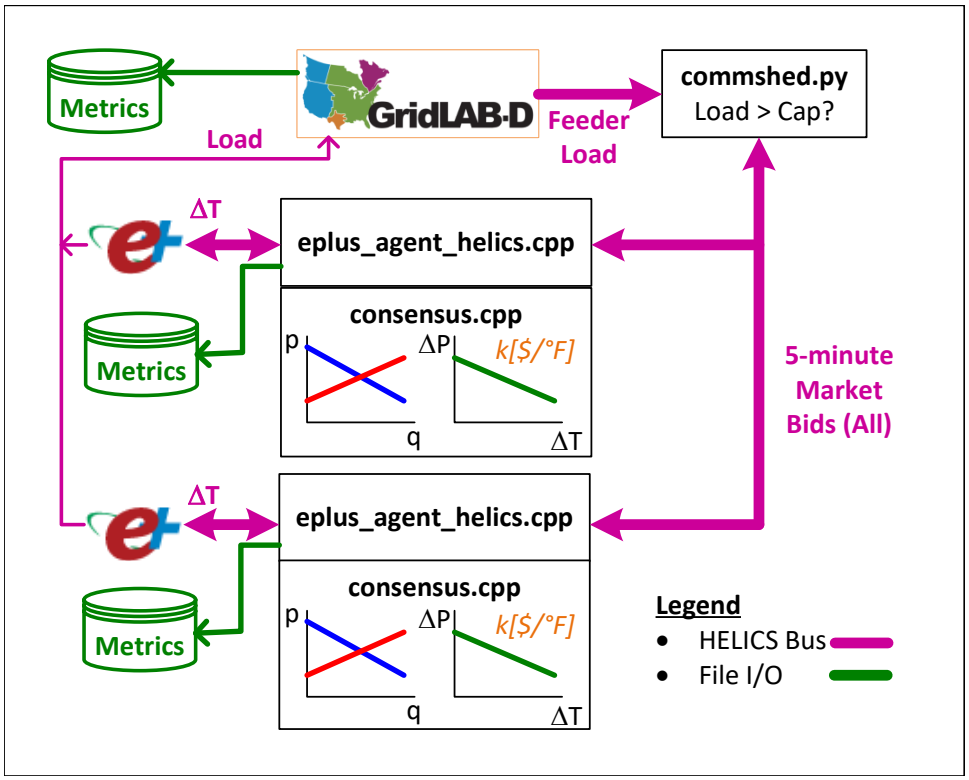

Figure 3. Consensus mechanism with GridLAB-D and EnergyPlus.

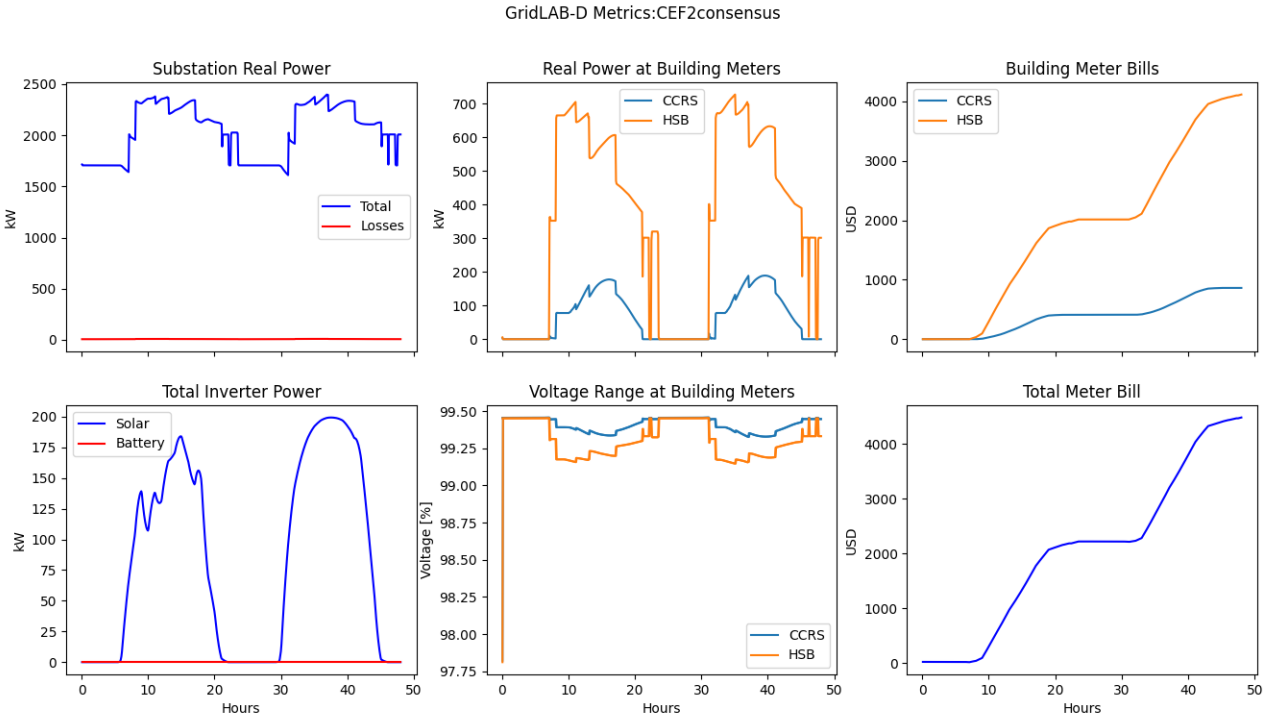

Figure 4. GridLAB-D outputs from consensus mechanism simulation.

expected in the real building. The $Setpoint$ may differ from $Schedule$ due to price response of the thermostats. The building HVAC system tries to maintain $Actual$ air temperature at the $Setpoint$. When the $Actual$ would exceed $Setpoint$, the $Cooling$ loads turn on. These comprise most of the $Total$ building electrical demand. Other components of demand are driven by the $Occupants$. When the $Setpoint$ exceeds the building's preferred $Schedule$, some occupants may experience $UncomfortableHours$ as defined by American Society of Heating, Refrigerating and Air-Conditioning Engineers (ASHRAE). EnergyPlus outputs this as a performance metric.

The right-hand column of Figure 5 shows the consensus market response to a utility request for flexible load reduction of up to 200 kW. The CCRS is able to clear approximately 35 kW of this request, at the price of $150/MWhr. That amount is limited by the maximum thermostat adjustment of 5 degF. We estimated the CCRS response by simulating its EnergyPlus model with setpoint changes of 1, 2, 3, 4, and 5 degF, recording the changes in building electrical demand. As a comparison, the $Real-timePrice$ in Figure 5 may represent a fixed time-of-use rate structure, with a three-to-one price difference in peak to off-peak rates, i.e., $30/MWhr compared to $10/MWhr. Under the assumptions of this example, the consensus mechanism price must be five times higher than the fixed peak rate, to achieve a load reduction of 35 kW. That reduction is about 17% of the CCRS peak load. The consensus price should not reach that level every day. Otherwise, the utility would consider investing to increase Cap in Figure 3.

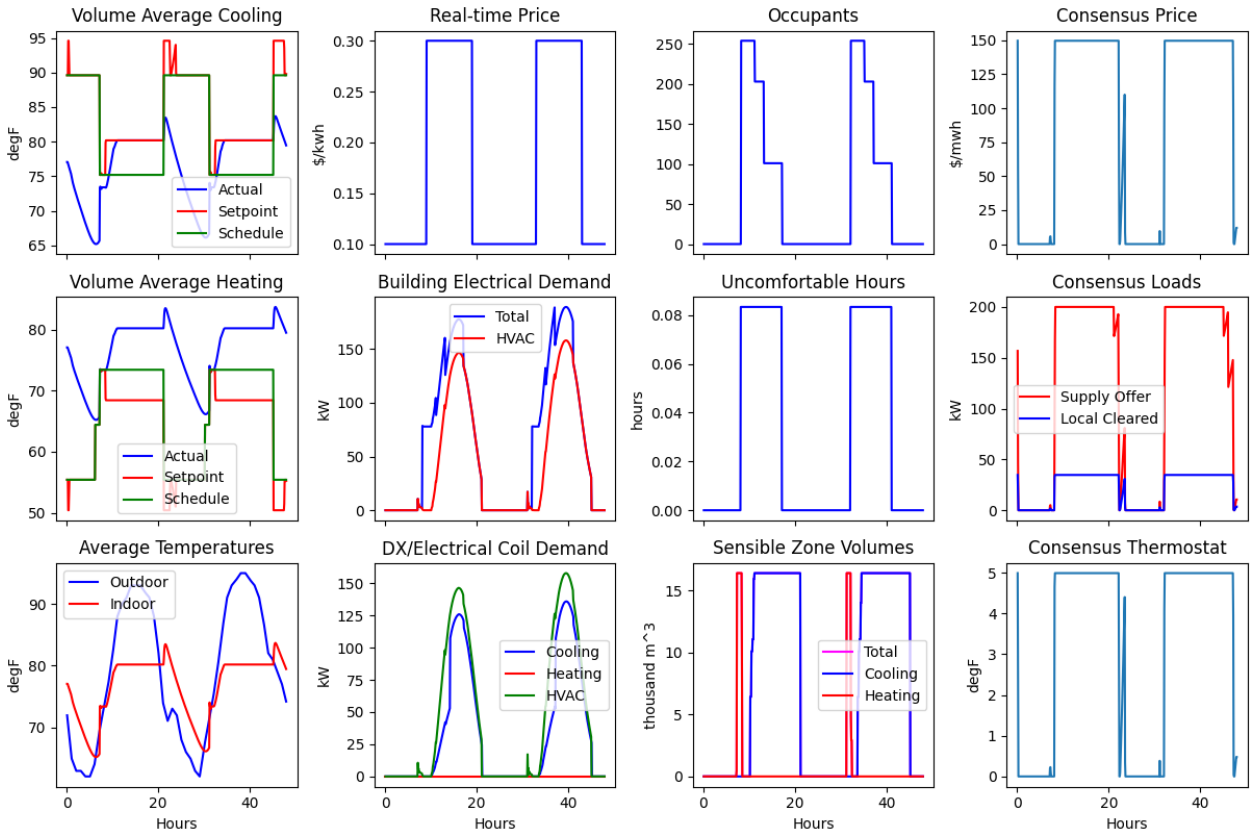

Figure 5. CCRS EnergyPlus outputs from consensus mechanism simulation.

Figure 6 shows the HSB EnergyPlus model response in the two-day TESP simulation. The definition of variables is the same as in Figure 5. The utility request is 200 kW and the cleared price is $150/MWhr, as in Figure 5, but here the HSB is able to supply 62 kW of the request, or

9% of its peak load. Together, the CCRS and HSB supply 97 kW load reduction, or less than half of what the utility requested.

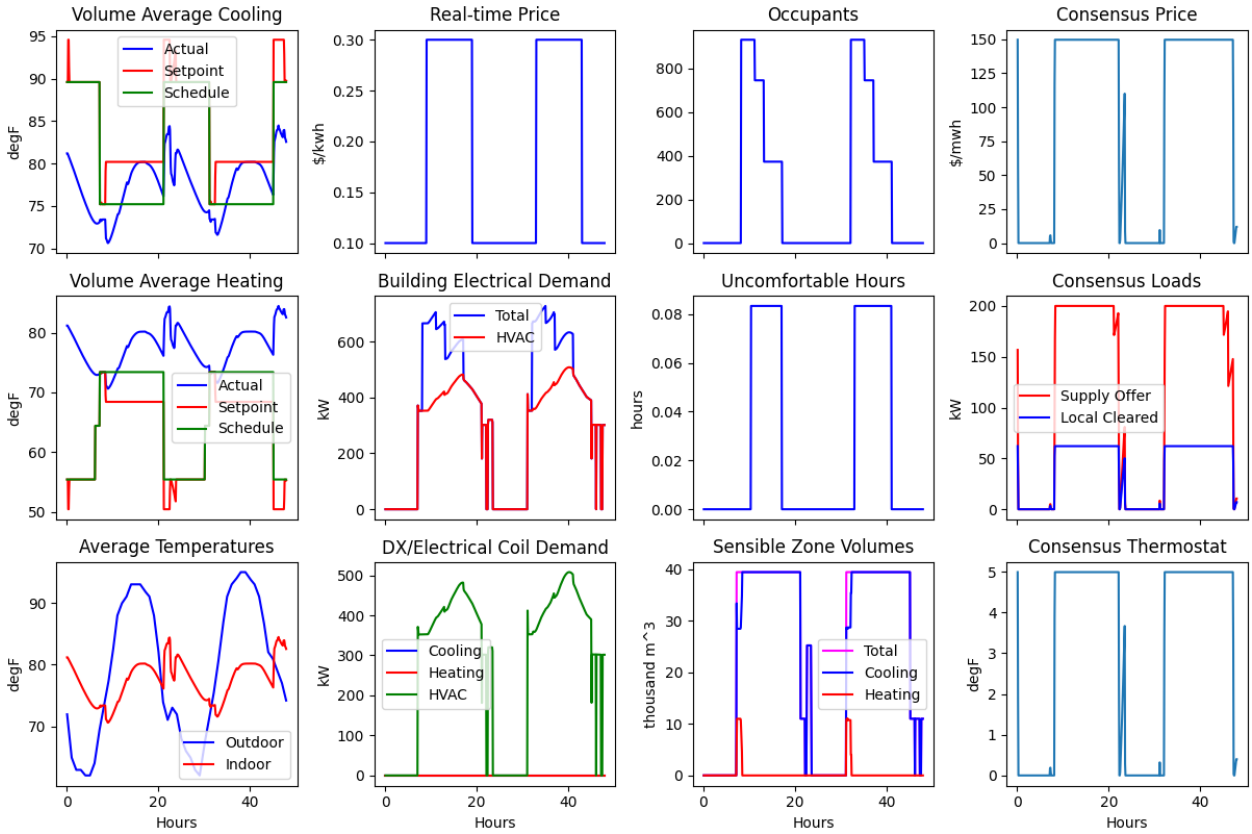

Figure 6. HSB EnergyPlus outputs from consensus mechanism simulation.

PNNL provided both EnergyPlus models to WSU's project team for their simulation work. PNNL then sought an improved building model for additional work on the consensus mechanism with virtual batteries, to address these shortcomings in the EnergyPlus model:

1. Dependence on assumptions for HVAC details, building occupancy, etc.
2. Dependence on a 3D drawing of the building, and material properties.
3. No information provided on reactive power.
4. No separation of building load into 208V and 480V components, which are separately metered.
5. Limitations on time step, i.e., no less than 5 minutes.
6. Initialization time for EnergyPlus to "warm up".

The data-driven model is described in [5]. It is based on sub-minute electrical data from the feeder, and separate building meters at 480 and 208 volts. We supplemented this with 5-minute weather data on solar radiation, temperature, wind speed, and humidity from [6], and 60-minute weather data on pressure from [7]. Figure 7 shows the building meter data, down-sampled to

the same 5-minute interval as the weather data. Two noticeable gaps in the data appear; these most likely correspond to electrical outages on those dates.

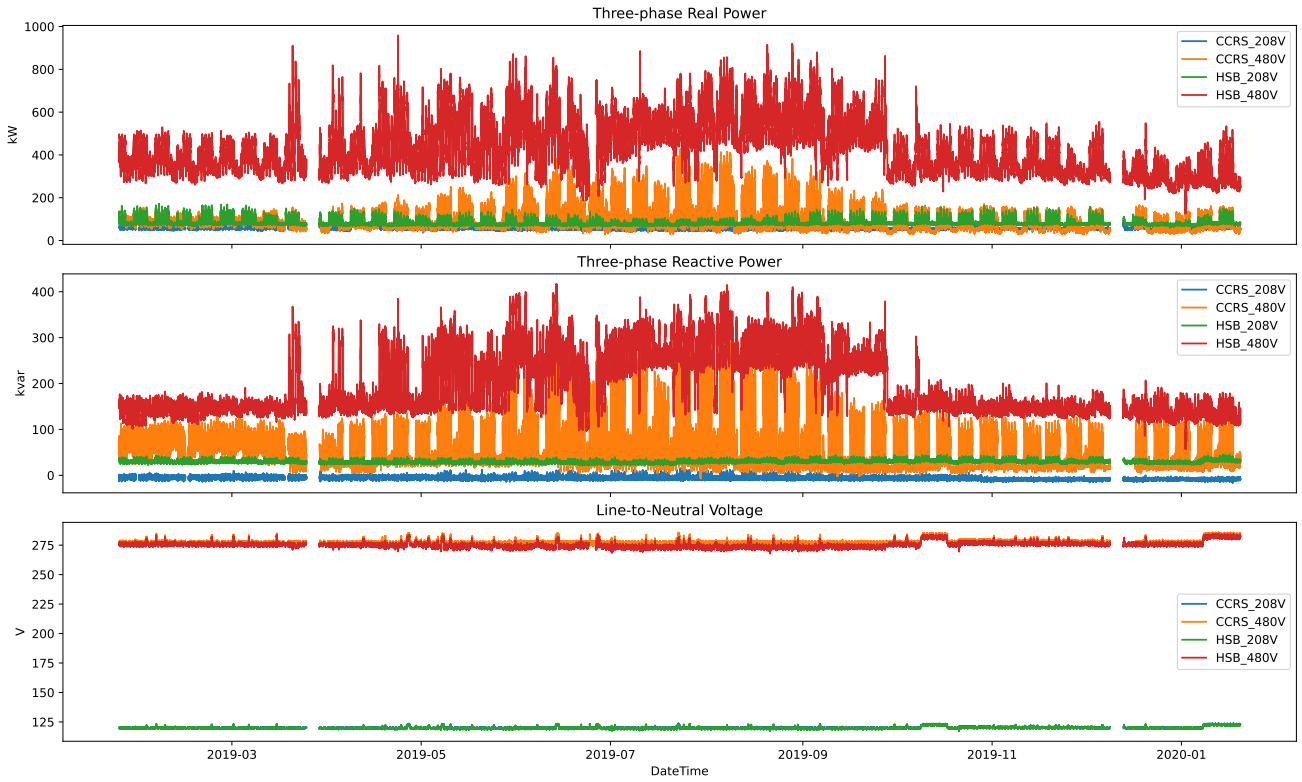

Figure 7. Building meter data from 2019, down-sampled to 5-minute intervals.

3.0 Transactive Energy Simulation

3.1 Feeder Modeling

The feeder models came from [8], plotted for GridLAB-D simulation in Figure 8. The combined model has four recloser segments among two feeders, 2574 three-phase buses, and approximately 10 MW of load at 582 buses. An OpenDSS [9] version of the feeder model is also available.

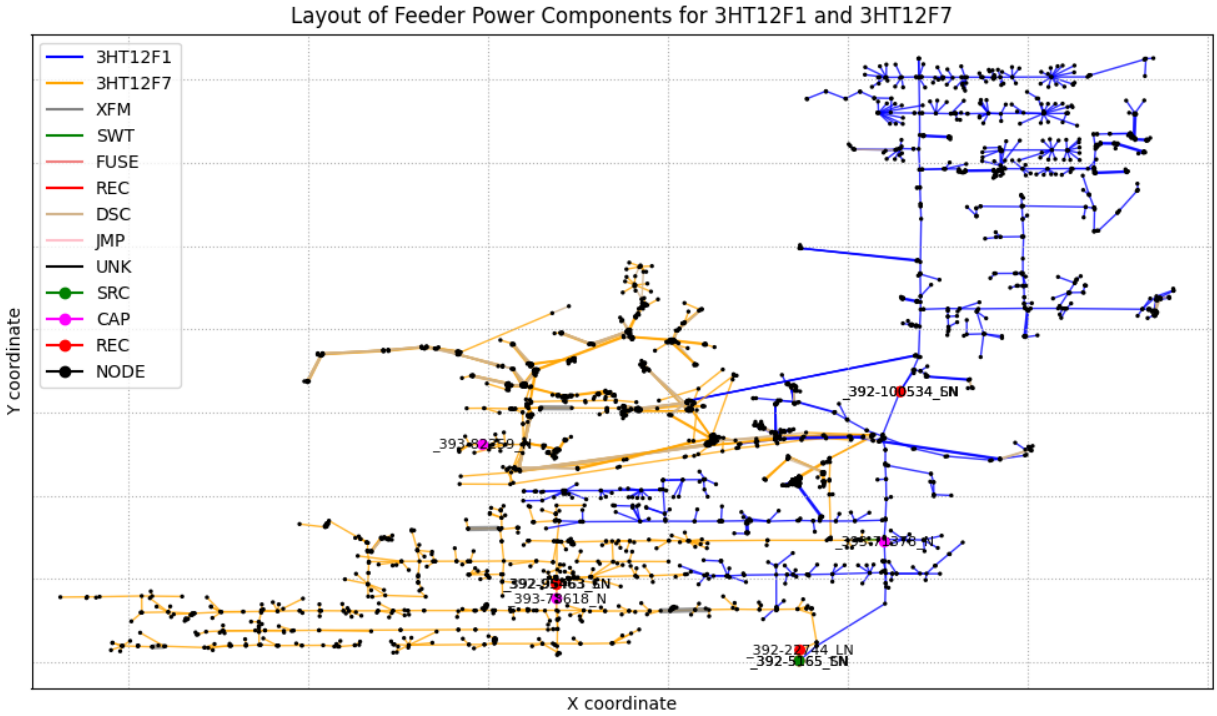

Figure 8. Full-order model of the feeders supplying CEF2 microgrid from CIM.

We reduced the model order to Figure 9 for transactive microgrid simulations. This reduced-order model matches the impedance seen at the PCC, and the total load external to the PCC, while retaining details inside the SEE microgrid. Compared to Figure 8's 2574 buses, the model of Figure 9 has 54 buses. Table 2 summarizes the component counts from Figure 9. There are two feeders that may supply the microgrid, from two different 30-MVA transformers in the same substation. Normally, feeder 12F7 supplies the microgrid. Within the microgrid section, Figure 9 includes drawings of the EnergyPlus models for HSB (top) and CCRS (bottom). The house symbols in Figure 9 represent variable feeder load outside the microgrid.

Figure 10 shows the final reduced-order model of the CEF2 SEE project used for transactive mechanism simulations. Components outside the automated transfer switch (ATS) represent the variable load on feeder 12F7 apart from the microgrid, and the equivalent impedance at the

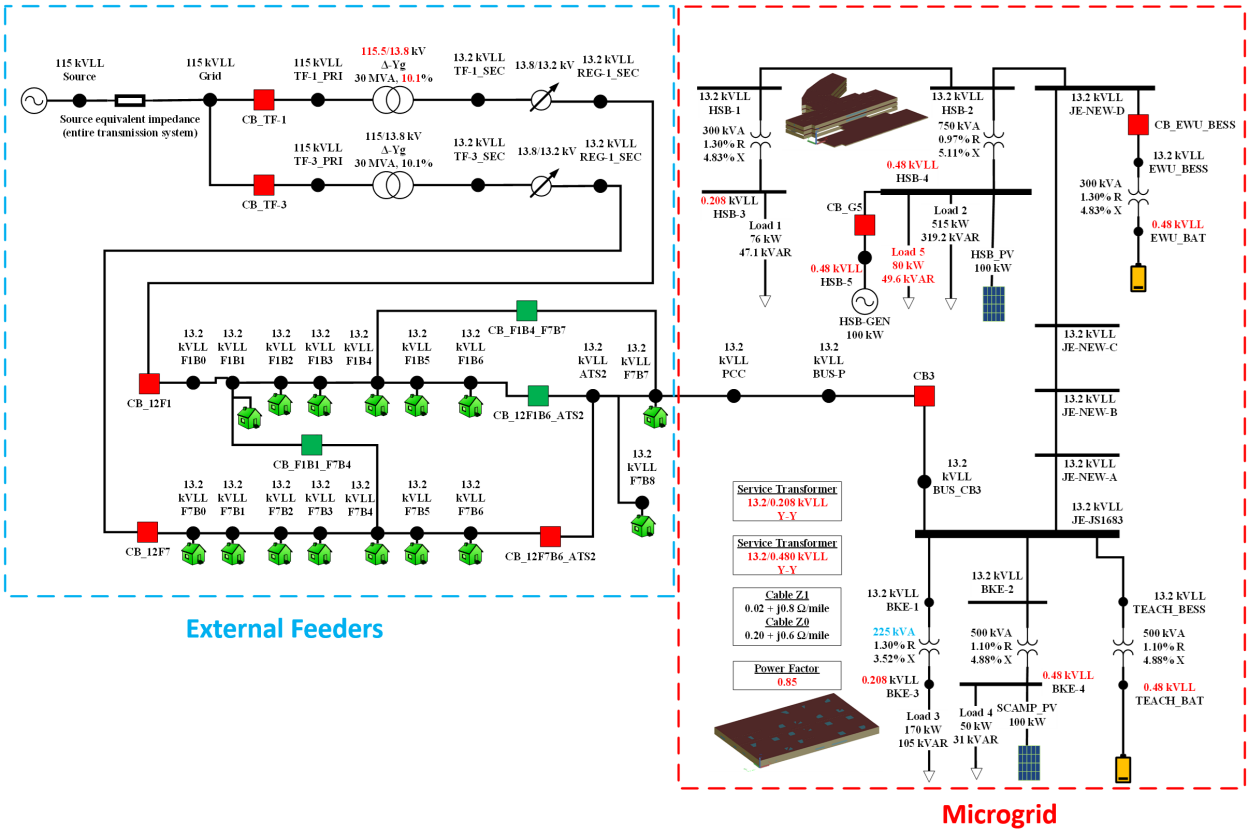

Figure 9. Details of the CEF2 SEE microgrid, supplied from one of two external feeders.

Table 2. Simplified Circuit Model Components

Class	Count
Substation Transformers	2
Regulators	2
Diesel Generators	1
Photovoltaic (PV) Systems	2
Battery Energy Storage Systems (BESS)	2
Spot Loads	5
House Groups	14
Houses per Group	42
Tie Switches	3

ATS. In this model, the ATS is the PCC. The same weather drives the house models, building models, and PV generators in the microgrid. The two PV generators are on the CCRS and HSB rooftops. The two BESS, labelled Eastern Washington University (EWU) and TEACH, are at different campus buildings.

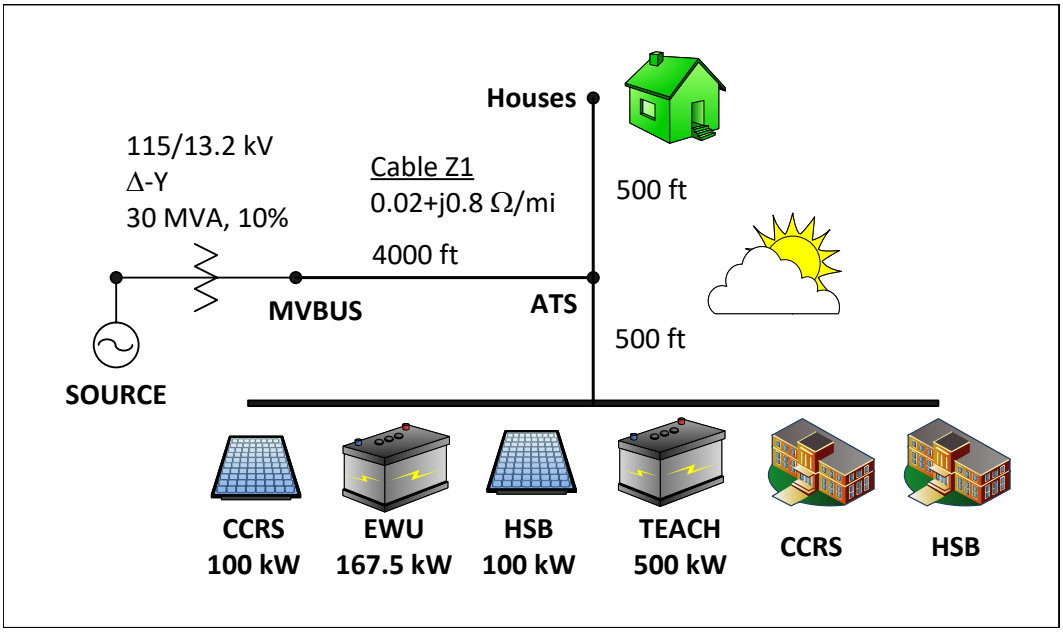

Figure 10. Reduced-order model of the CEF2 microgrid for transactive energy simulations.

Figure 11 depicts the house model in GridLAB-D [10] with other behind-the-meter resources, including PV and BESS. The house model includes a second-order thermal equivalent circuit to represent the house heating and cooling in response to a thermostat-controlled HVAC system. End-use appliances and lighting loads switch on and off, in response to randomized occupant schedules. This house model resembles the EnergyPlus model, but with a single HVAC zone and with building thermal performance simplified to a second-order circuit. We simulated the feeder with 588 of these house models to obtain a record of variable house loads during two summer days. This record provided a feeder base load. The CEF2 SEE microgrid resources in Figure 10 add to or subtract from this base load. The house loads make the total feeder load higher than in Figure 4, so that the hypothesized market will have a more interesting test scenario.

3.2 Virtual Batteries in Consensus Mechanism

The consensus mechanism is based on [11]. The virtual battery (VB) is based on [12]. Figure 12 shows the design of a Python-based agent to expand the stock TESP agents shown in Figure 3. The new features are VB subclasses for $Building$, $Battery$, and $Photovoltaic$ to manage the common VB attributes for energy and power. See [5] for more details, including the machine learning (ML) model developed for the $Building$.

Figure 13 illustrates the VB and consensus mechanism response to simple $Price$ stimuli, plotted in the upper right. In simulated real time, the BESS discharge during times of high price, and charge during times of low price. When the price is above a base level of $0.207, the BESS discharge at a rate determined by 500 kW/$ for EWU, and 1500 kW/$ for TEACH,

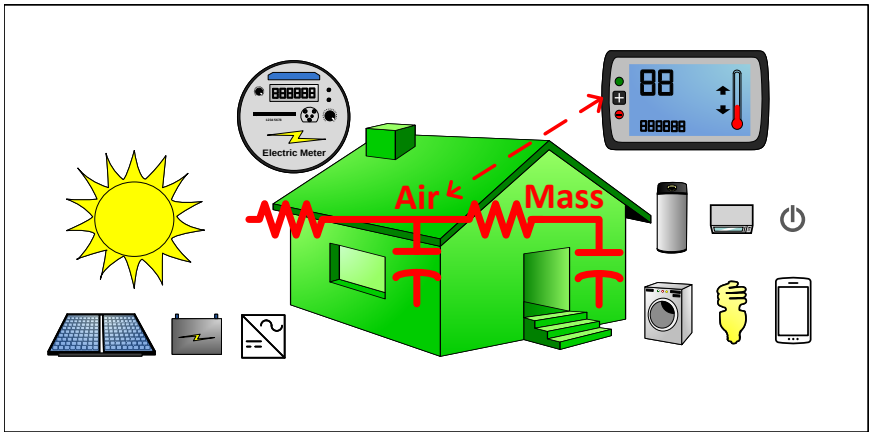

Figure 11. House model with HVAC system and behind-the-meter resources in GridLAB-D.

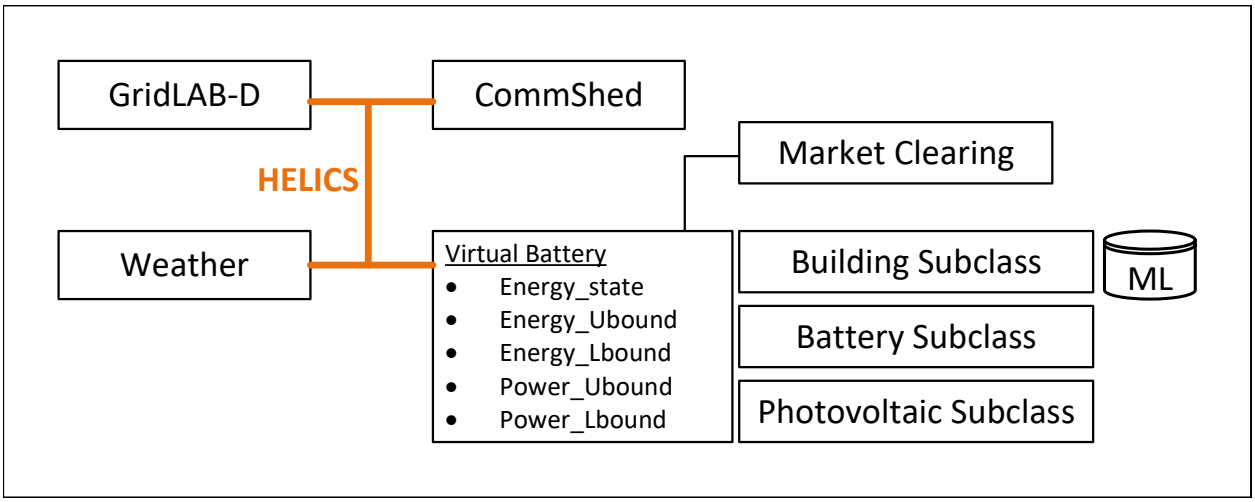

Figure 12. Virtual battery agent and simulation federates (GridLAB-D, Weather, CommShed) linked through HELICS, with machine learning (ML) option for commercial buildings.

subject to inverter limits and state of charge. Similarly, the buildings may decrease their base loads in response to prices above $0.207. These power levels are plotted in the upper left, as market participants. The utility is not directly a participant, since the price variations with time of day are pre-determined. In this example, and those to follow, prices and the DER price responses were just chosen to provide clear illustrations.

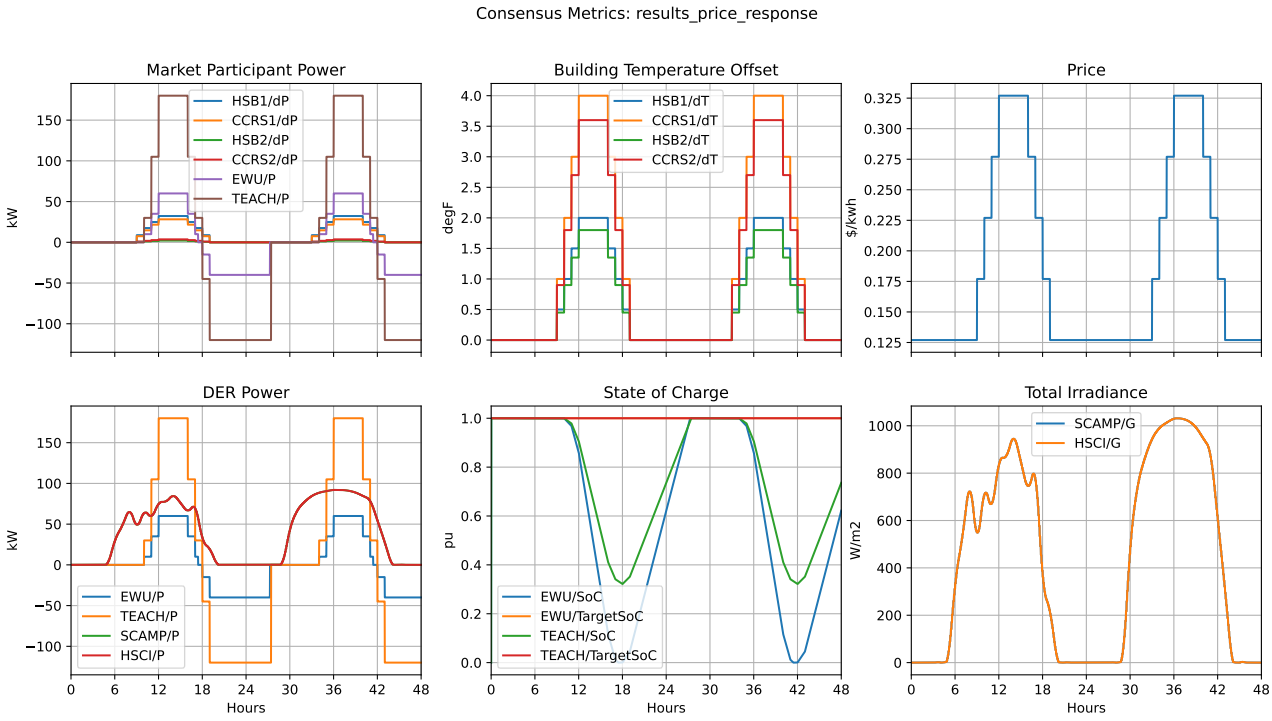

Figure 13. Time-of-day pricing results for the DER participants, batteries fully charged.

In this section of the report, we replaced EnergyPlus in TESP with results recorded in Section 2.0. With reference to Figure 12, the Building Subclass reads baseline building load values vs. time from disk files. One reason was to improve simulation time. Another reason was to separate 208V from 480V loads in each building, based on data from separate revenue meters. We could then simulate building response as deviations from the baseline values. We could also replace the baseline EnergyPlus results with a data-driven model that responds to different weather and occupancy conditions.

The building response is determined first from a temperature response coefficient, k, shown in Figure 3. The temperature response is then translated to a power response using a lookup table of EnergyPlus simulation results. The lookup table was generated by running sets of EnergyPlus simulations at different thermostat settings, and taking the difference of the results. Table 3 summarizes the building demand response to thermostat setting changes inferred from these EnergyPlus simulations. The 480V responses are higher because the HVAC systems connect at that voltage level. (The last row, at 10 degF, is based on load shed tests reported later, not on the EnergyPlus simulations.) In the case of Figure 13, k for $HSB1/dT$, the 480V load, is assumed to be $10/degF. Between hours 12 and 16, the price is $0.327, or $0.200 over the base price. Therefore, $HSB1/dT$ is 10 degF between hours 12 and 16. According to Table 3, $HSB1/dP$ should be 25.72 kW between hours 12 and 16, which appears to be the case in the plot of Market Participant Power. The sign convention is positive for BESS discharge and

for building load reduction. The buildings will not increase load in response to price, but the BESS may charge in response to price, so BESS Market Participant Power can be negative. In Figure 13, the k values were exaggerated and differentiated for illustrative purposes, as were the BESS price response coefficients.

Table 3. Imputed Building Power Response to Thermostat Settings in August

ΔT [degF]	CCRS ΔP [kW]		HSB ΔP [kW]	
	208V	480V	208V	480V
0	0	0	0	0
1	-1.00	-7.42	-0.96	-13.90
2	-2.00	-14.65	-1.92	-25.72
3	-3.00	-21.59	-2.88	-35.17
5	-5.00	-34.72	-4.80	-49.66
10	n/a	-64.00	n/a	-144.00

The two PV installations do not respond to price, neither here nor in any other cases in this report. Both have identical outputs, plotted in the lower left where $SCAMP/P$ and $HSCI/P$ overlay each other. Each PV experiences the same total irradiance, plotted in the lower right. On the second day, G can exceed 1000 because it includes both direct and diffuse irradiance. Both BESS begin fully charged. Even though EWU/P is lower than $TEACH/P$, the EWU/SoC reaches zero because its physical storage capacity is less than represented by $TEACH/SoC$. When not discharging, both BESS try to regain their $TargetSoC$ values. These SoC variations are plotted in the lower center of Figure 13.

Figure 14 adds the utility request for responsive load, which is made whenever the substation load exceeds 4000 kW, subject to a cap of 400 kW. The peak load is about 4671 kW without the market, so if a 400-kW purchase offer were fully subscribed, the peak might be reduced to 4272 kW. As shown in the upper left plot, only about 252 kW of the utility offer is cleared in the market. The two BESS supply around 200 kW, with almost 50 kW supplied from load reductions at the two buildings. The clearing price is about $0.46/kwh when all four DER participate. However, first EWU and then TEACH batteries completely discharge. After that happens, the cleared price increases to about $0.80/kwh and the buildings combine to clear about 81 kW at the higher price. Under local control, the BESS begin to recharge when the market price drops below $0.207/kwh, so the BESS charging does not exacerbate the substation peak load. Increasing the target SoC could allow the BESS to participate for a longer time, but there may be other factors influencing the target SoC.

The utility offers to buy power according to a demand curve that ramps from $0.127/kwh, at 0 kW, to $1.00/kwh at 400 kW. The BESS offer to sell into the market at prices that ramp from $0.207/kwh, at 0 kW, to $0.60/kwh at 100 kW (EWU), or $1.20/kwh at 500 kW (TEACH). If the utility offered a higher price, or the DER offered lower prices, then more of the 400 kW request would be cleared in the market.

Figure 15 shows the distribution system response to the VB consensus simulation that produced Figure 14. To the upper left, the green plot of $Houses$ represents the record from simulation of 588 houses modeled as in Figure 11. The peak substation load is about 4424 kW, which is 247 kW less than the pre-market peak of 4671 kW. Recall that the market cleared 252 kW, but due to losses, voltage dependencies of load, and timing mismatches, only 98% of the

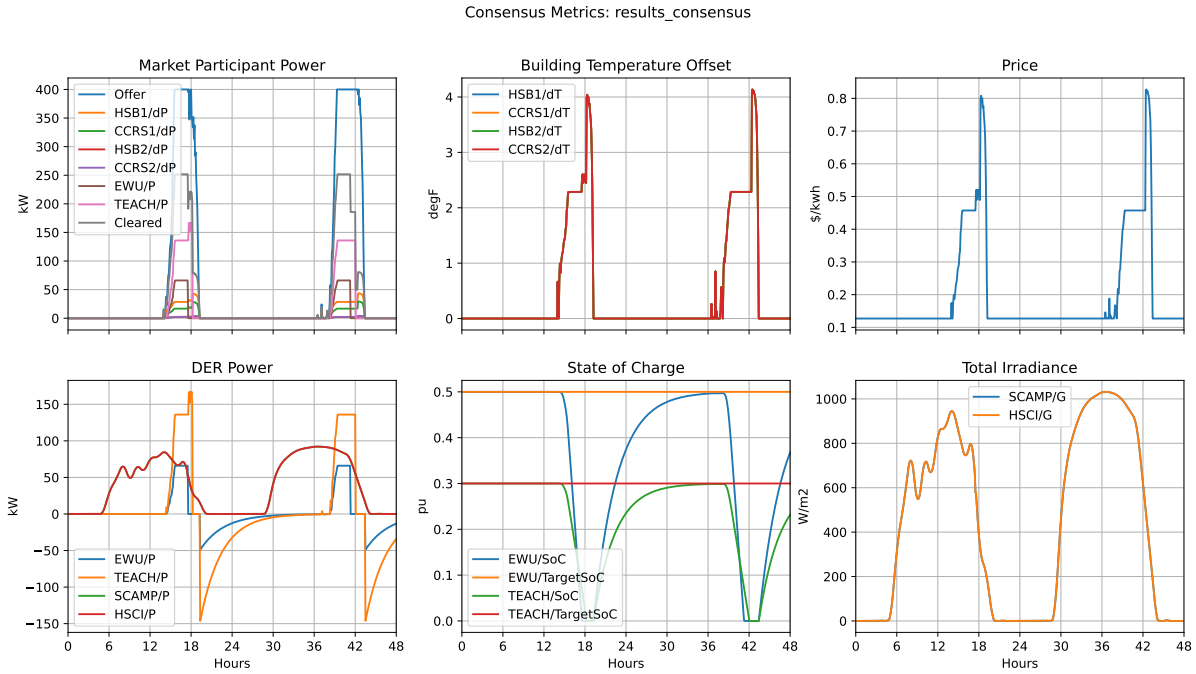

Figure 14. Consensus results for the DER participants; EnergyPlus buildings.

cleared amount reduces the substation peak load. The top center plot shows CCRS and HSB loads separated into 480V and 208V components, where the 208V component is approximately constant and significantly less than the 480V component. The data-driven model, described later, may represent the separation more accurately. In the right-hand plots of meter billing, there is an initial fixed fee of $250 per meter, after which the totals increase monotonically over two days.

Figure 16 represents the distribution system response with no VB, no BESS operation, and no consensus mechanism. In comparison to Figure 15, this pre-market peak substation load is higher, at 4671 kW. The daily peaks occur at approximately 1700 hours. The second day's peak is slightly higher than the first day's peak, as the higher PV output is more than compensated by the higher weather-driven house and commercial building loads. The substation load is comprised of houses, commercial buildings, solar generation, and some constant spot loads. The BESS do not operate.

Figure 17 shows the baseline response of data-driven building models, with temperature, voltage, feeder current, and day-of-week, and occupancy inputs [5]. In comparison to Figure 16, the pre-market peak substation load is 4577 kW. Note that the data-driven model is calibrated against meter and weather data directly, not against the EnergyPlus models. Comparing the top center plots in Figures 17 and 16, the data-driven model exhibits more plausible variation in both 208V and 480V loads.

Figure 18 represents the DER participant responses in a consensus market, with the data-driven CCRS and HSB models. Using the same price and building response assumptions, the market clears 252 kW as in Figure 14, even though the underlying baseline building loads are different.

Figure 19 represents the distribution system response, with a consensus market mechanism and the data-driven building models. The peak substation load is 4334 kW, which is 243 kW less than the pre-market peak of 4577 kW. The data-driven building models have more voltage

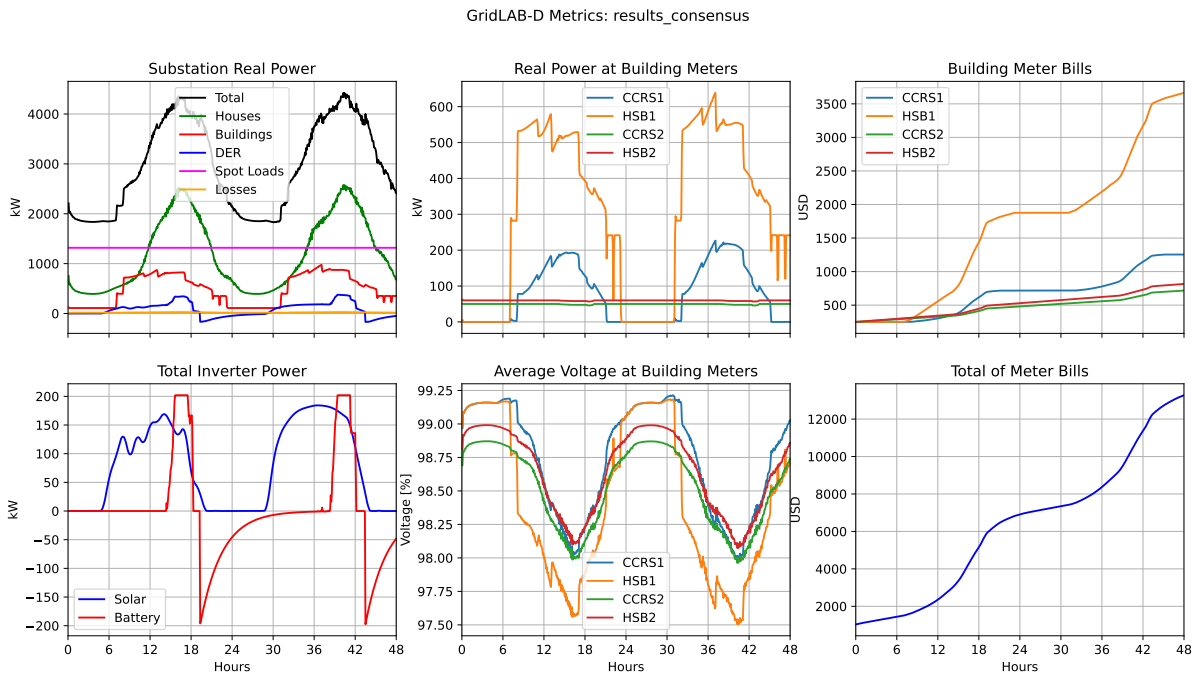

Figure 15. Consensus results for the distribution system; EnergyPlus buildings.

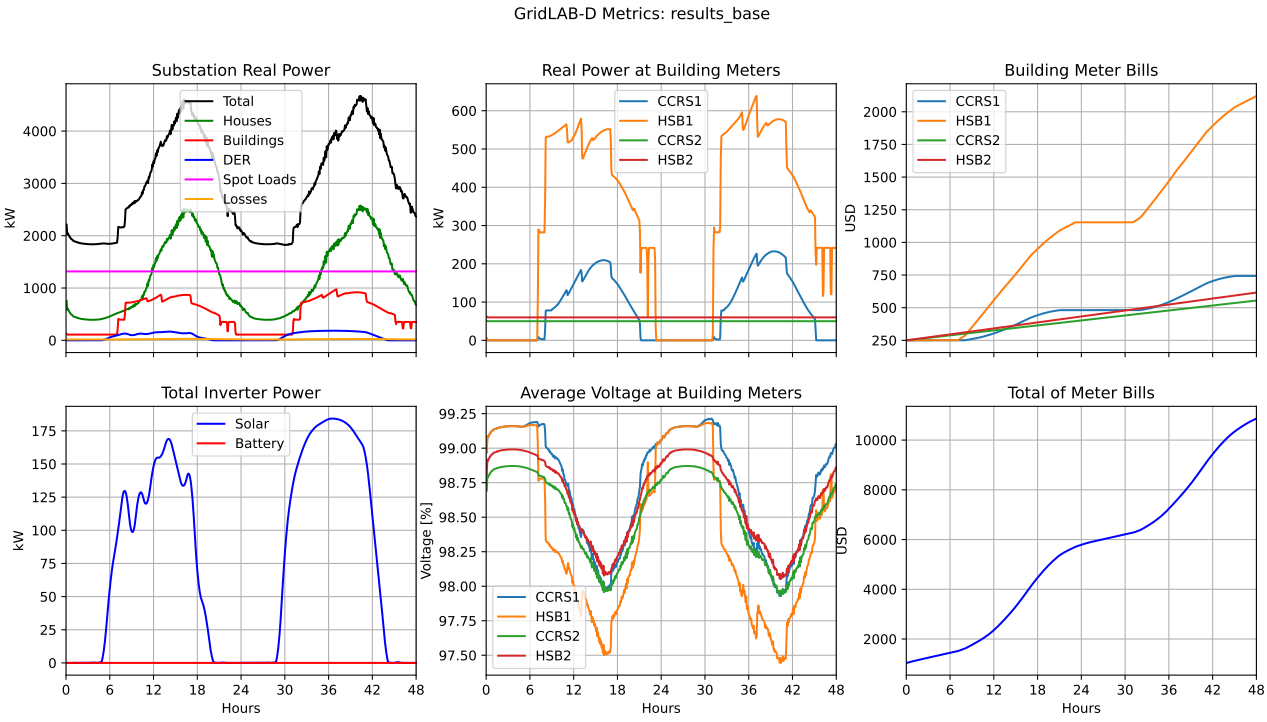

Figure 16. Base load with EnergyPlus/House player files and fixed prices in GridLAB-D.

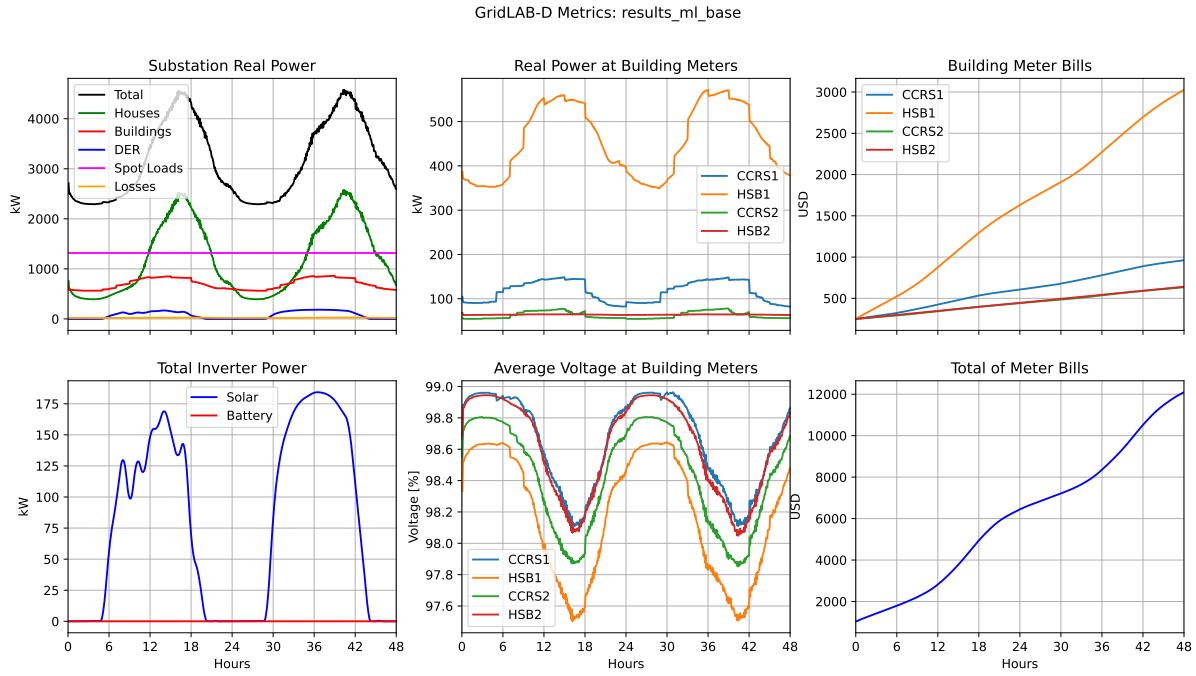

Figure 17. Distribution system response with data-driven buildings and fixed prices.

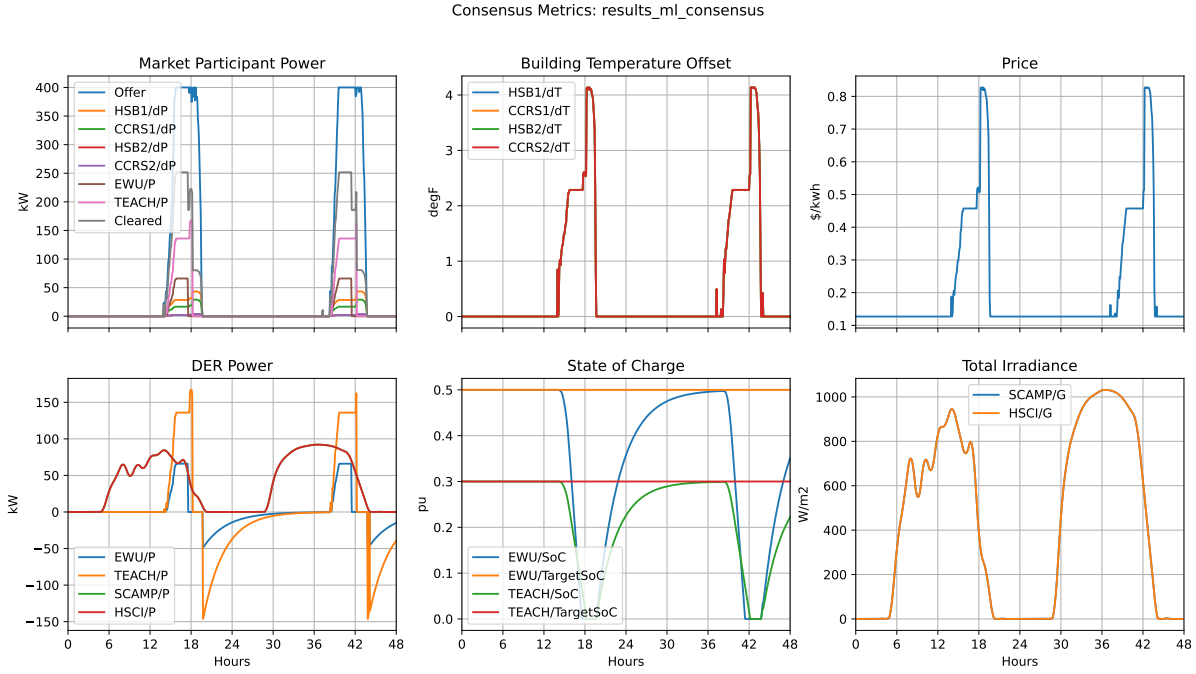

Figure 18. Consensus results for the DER participants; data-driven buildings.

dependency than the EnergyPlus models. When the substation peak load decreases, the load voltages tend to increase, which increases the data-driven loads. That partially counteracts the market action, so only 96.4% of the cleared amount results in a substation peak load reduction.

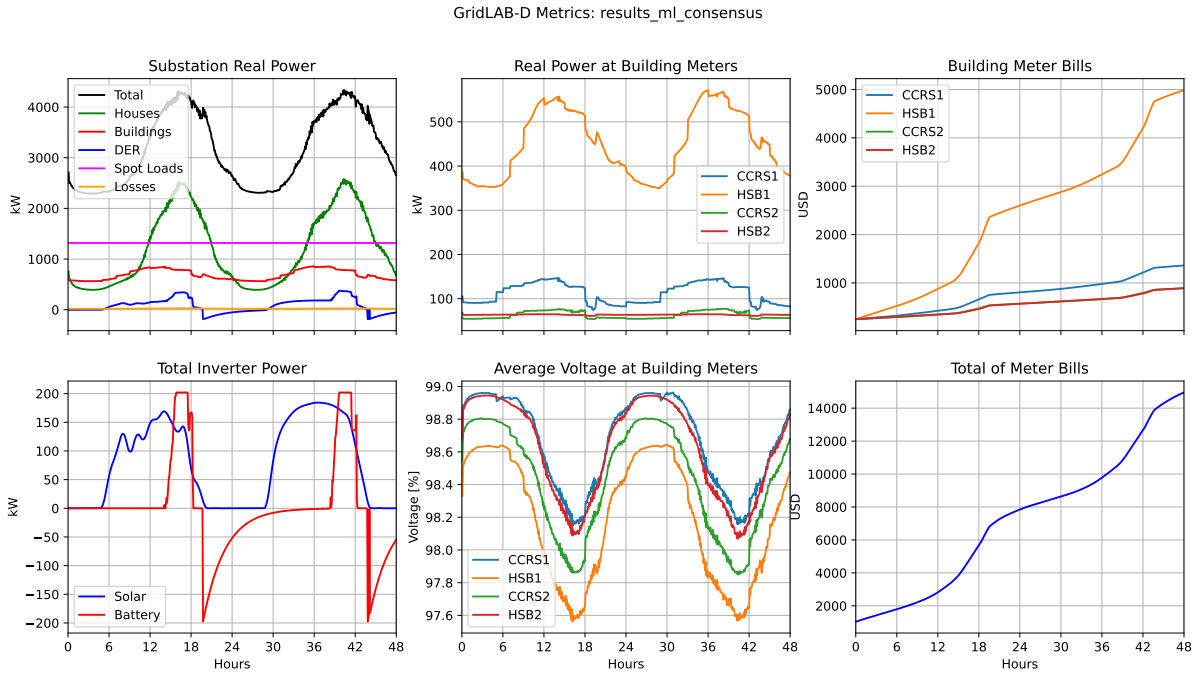

Figure 19. Consensus results for the distribution system; data-driven buildings.

Figure 20 represents the DER participant response and Figure 21 represents the distribution system response with time-of-day rates, and the data-driven building models. The BESS operate in a price-driven cycle to fully charge and fully discharge each day. Similarly, the buildings reduce load each day in response to hourly price changes. The sum of maximum response is about 313.8 kW, but that occurs between 1200 and 1600 hours each day, when prices are highest. The substation peak load occurs after that window, at around 1700 hours. As a result, substation peak load reduces from 4577 kW (Figure 17) to 4457 kW (Figure 21), a difference of 120 kW. Only 38% of the maximum time-of-day response helped to reduce the substation peak load. The obvious fix would be to shift the peak pricing window later in the day, to cover early evening hours. However, the consensus mechanism is still more adaptable to changing grid, load, and especially BESS conditions.

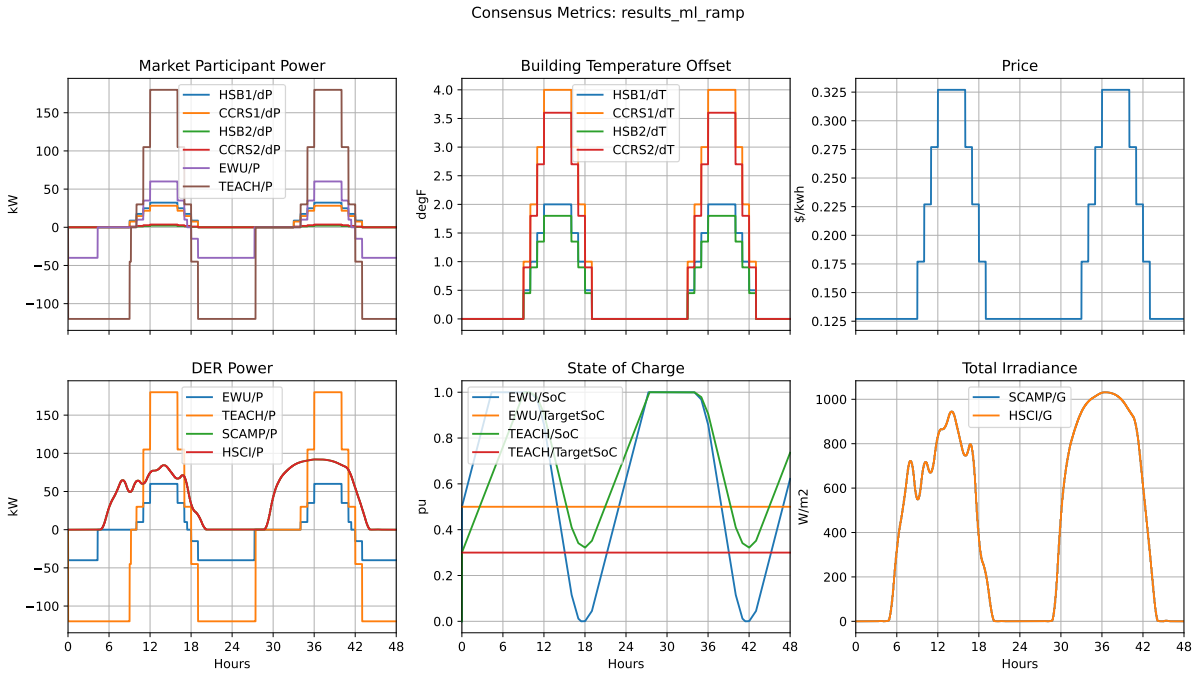

Figure 20. Time-of-day pricing results for the DER participants; data-driven buildings.

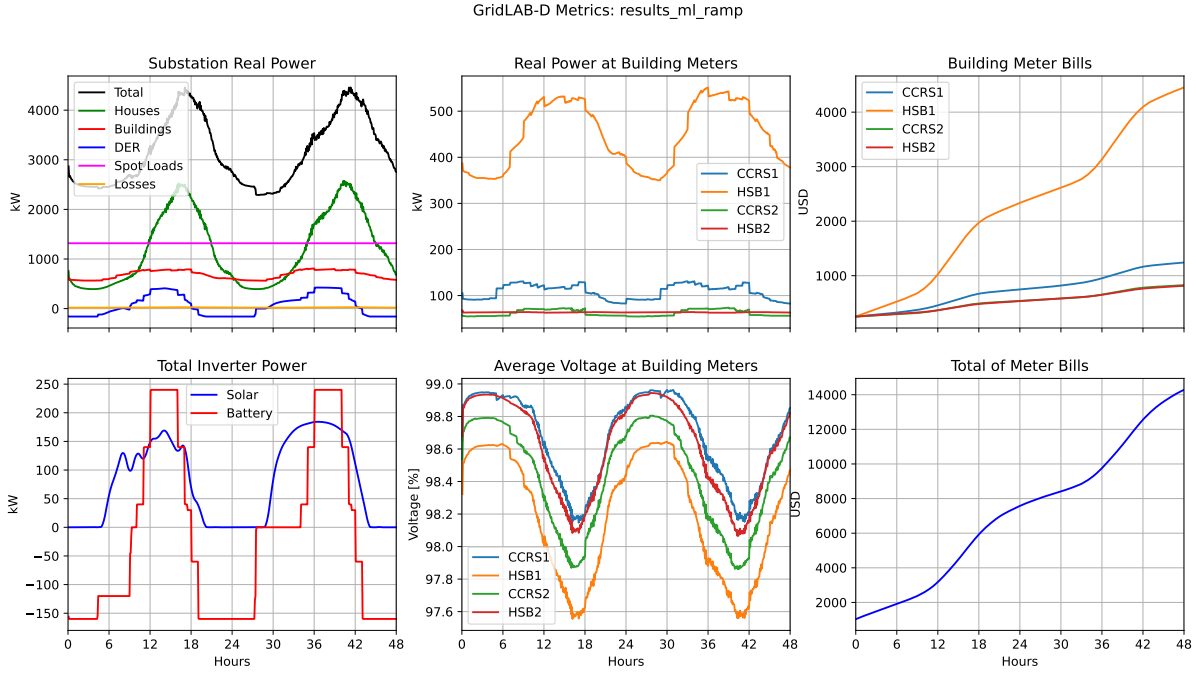

Figure 21. Time-of-day pricing results for the distribution system; data-driven buildings.

4.0 Use Case Testing

Avista performed use case testing to satisfy requirements of their contract with WA Department of Commerce (DOC), as summarized in that contract's Attachment C:

1. Grid Services: Load Shaping, Frequency Regulation, Ramping/Balancing, Distribution Efficiency, Power Quality
2. DER Optimization: Solar Optimization, Local Battery Optimization
3. Building Fleet Optimization: Demand Optimization, Demand Response
4. Critical Resiliency: Islanded Operation, Critical Load Resiliency, Peer-to-Peer Market Transaction (simulation only using consensus mechanism), Reconnect to Grid

PNNL advised Avista on planning for tests to verify these WA DOC requirements, which may differ from those of the BESS techno-economic use case testing funded by DOE [13].

4.1 Test Planning

The tests were planned to satisfy all requirements of the four WA DOC use cases, with minimal disruption of Avista and WSU operations.

4.1.1 Test Scheduling

General considerations for sequencing and scheduling:

1. Two weeks commissioning period beginning July 12, 2021.
   a. First week was for installation and commissioning tests.
   b. Second week was for islanding tests (Critical Resiliency Mode). This would also verify operation of the microgrid controller.
2. Other mode (use case) tests could be scheduled for a later time, minimizing risks to WSU service.

4.1.2 Data Collection

These measurement types, locations, and settings applied to all tests:

1. HSB and CCRS building, PV, and battery meters are SEL 735 (for revenue and power quality applications), intermediate version, sampling at 3-second sample intervals.
   a. The SEL 735 triggers were set to capture event waveforms, which are especially significant during the islanding tests.

   b. These meters were networked to Avista's data historian in time for the tests.

2. Feeder SCADA data was collected at 10-second sample intervals.

3. Other sensor and data streams are specifically associated to the PCC, e.g., a SEL 451 protection control. Supplemental power quality monitors from Avista and PNNL, e.g., Fluke 435, were not needed.

4. Weather data was available at 5-minute (temperature, humidity, wind, solar) and 60-minute (pressure) intervals, from the NOAA site or Spokane airport.

5. On-site observers of HSB and CCRS occupancy and activity were considered. We would have needed to pre-arrange access to view building management system controls. In possible future tests, occupancy sensors may be available from PNNL, McKinstry or WSU.

6. These data sources would satisfy requirements for use case test reporting, and model/algorithm validation.

4.1.3 Critical Resiliency Testing Procedure

This test was originally planned for the week of July 19, 2021, but deferred to August 2021.

1. Planning considerations:
   a. The local synchronous generator owned by WSU did not participate, only the Avista-owned solar, batteries and microgrid controller.
   b. Considered daytime and nighttime tests for different solar availability.
   c. Reviewed yearly load profiles for probability of black starting without manual load reduction. Estimated the critical and non-critical loads before initiating the test.
   d. Solar output could have been curtailed if necessary.
   e. Avista documented a tabulation and switching plan for building internal critical and non-critical loads. An implementation was already programmed in the SEL controller but the quantities weren't verified or enforced, i.e., the controller works down a priority list of loads until it obtains the required response.
   f. Other options to match generation and load are to manually trip building panels, or run a single building in the microgrid.

2. Test sequence: start the microgrid with load/generation balance maintained, ride through all voltage and frequency deviations.
   a. Verify the batteries are at 80-90% SoC to provide some down-ramping margin as loads and possibly solar fluctuate.
   b. Turn off non-critical loads (these were actually stuck in the pre-outage state).
   c. Start the batteries, which forms the grid and picks up the building load.
   d. SEL load management logic will be on: estimate, monitor and verify the length of time microgrid operates with only critical loads.
   e. Connect the solar generation during daytime. This might not occur in time to support the grid at high load. The anti-islanding feature and connection time delay should have been disabled.

f. Run the island for 1-2 hours. The SEL controller should manage resources to achieve desired island operation time.
g. Reconnect to the grid feeders at the PCC.
h. SEL load management logic shuts down, and batteries change to grid-following real and reactive power dispatch.
i. Add non-critical loads to the buildings as the occupants demand.
j. This verifies all of the critical resilience use case, except for peer-to-peer transactions that were demonstrated by simulation in TESP.

3. Tasks for TESP simulation:
   a. Determine the pre-test range of battery SoC to maintain up and down reserve during the islanding test.
   b. Simulate peer-to-peer transactive operation under hypothetical market scheme.

4.1.4 Steady State Testing Procedure

These tests were designed to satisfy the first three WA DOC use cases in one procedure that minimizes testing time. These tests did not require coordination of off-grid operation with WSU Facilities, so there was more flexibility in timing them. Separate day/night, weekday/weekend, or in-school/out-of-school time periods were considered.

1. Planning considerations:
   a. These are all grid-connected modes.
   b. The team needed to determine the smart inverter functions available, and the process for switching between modes of operation in the field. Avista was able to ”practice” the tests in their lab, and verify capabilities of SEL and Spirae controllers to change the smart inverter functions.
   c. Solar inverters are manufactured by SMA.
   d. The battery warranty allows one full charge/discharge cycle per day, based on kwh throughput. But this applies over a 5-year period, so was not a restriction on testing.
   e. WSU agreed to three weeks of additional testing in August, to cover these use cases.
   f. WSU faculty returned July 12, students returned August 18, school started August 25.
   g. Avista operations don’t restrict battery or PV dispatch.

2. Scenarios included:
   a. Load Shaping: impose an import (or export) limit at the PCC from the substation. Monitor compliance via manual switching of building loads, and microgrid controller operation of the batteries.
   b. Frequency Regulation: in CEF2 SEE, this means providing a dispatchable secondary control reserve from the batteries.
   c. Ramp/Balance: in CEF2 SEE, this means providing a dispatchable tertiary control reserve from the batteries. Points b and c may be combined with a, if the batteries maintain reserves throughout the combined test sequence.

d. Distribution Efficiency: demonstrate ability to control Q at the PCC, and monitor its effect on voltage at PCC and other monitored feeder locations. These should be step changes in Q, large enough to have a noticeable impact on voltage. Compare this to tap changes at the substation, dispatched from the Avista distribution management system (DMS). Energy savings, especially the losses, are to be estimated from simulation.

e. Power Quality: power factor correction is combined with item d because it involves control of Q. Engage smart inverter functions on the inverters (battery and solar) to manage voltage fluctuations (either manual mode change on site, or by simulation). The voltage changes in response to ΔQ at different voltage levels can help validate the feeder model, as described in Section 4.2.

f. Solar Optimization: change thermostat controls and non-critical loads to match the building load profile to solar output. This test is best done on weekends in daytime. This is a variant of item a, load shaping, except the batteries should not be involved.

g. Battery Local Optimization: this is how Spirae's controller operates by default, to minimize the building's demand charge on the monthly bill. For example, charge at maximum PV output, discharge at building peak load. Test by letting Spirae operate the batteries for an input tariff, and see how well it works.

h. Demand Optimization: for the pair (fleet) of buildings, this is demonstrated the same way as in f or g.

i. Demand Response: for the pair (fleet) of buildings, this is demonstrated the same way as in h, except that the source or basis of the control signal is different.

3. **The common element for most of these steady-state tests is to demonstrate the ability to follow a load shape.** The differences are whether a) batteries, buildings, solar or combinations of them participate and b) the rationale for the load shape. Only a) matters for testing. The test plan should include a minimal reference set of load shapes that cover all use cases.

4. Reactive power and smart inverter function testing, items d and e, could be separated. They might be done during the commissioning tests, along with ΔQ testing for model calibration. Simulation can be used to verify benefit of the smart inverter functions.

4.2 Effects of Reactive Power Change at the PCC

Figure 22 shows a simplified, positive sequence Thevenin equivalent at the PCC. The impedance value, $R + jX$, was obtained from the Z_{sc} function of an OpenDSS model of the feeder. The X/R ratio at no load is 4.79. At a load of 6 MW, unity power factor, the equivalent impedance may include a shunt resistance, shown in red. The "full load" equivalent impedance would be 0.347+j1.351, with a lower X/R ratio of 3.89. For short-circuit calculations, the no-load impedance is appropriate. For DER-induced voltage fluctuations, the full-load impedance may be appropriate because the loads are not short-circuited during normal DER operation.

Table 4 shows that a full-range ΔQ should produce only 0.5% ΔV at the PCC. The value of ΔQ is 667.5 kVAR, which represents a contribution from both batteries from zero to full absorption or full injection. In this case, the system is relatively strong, and the X/R ratio is relatively high, compared to typical distribution systems. Therefore, the simplified and exact formulas for d in Figure 22 give essentially the same result. The full-load condition also has little practical effect. That isn't necessarily the case for weaker DER interconnections or lower X/R

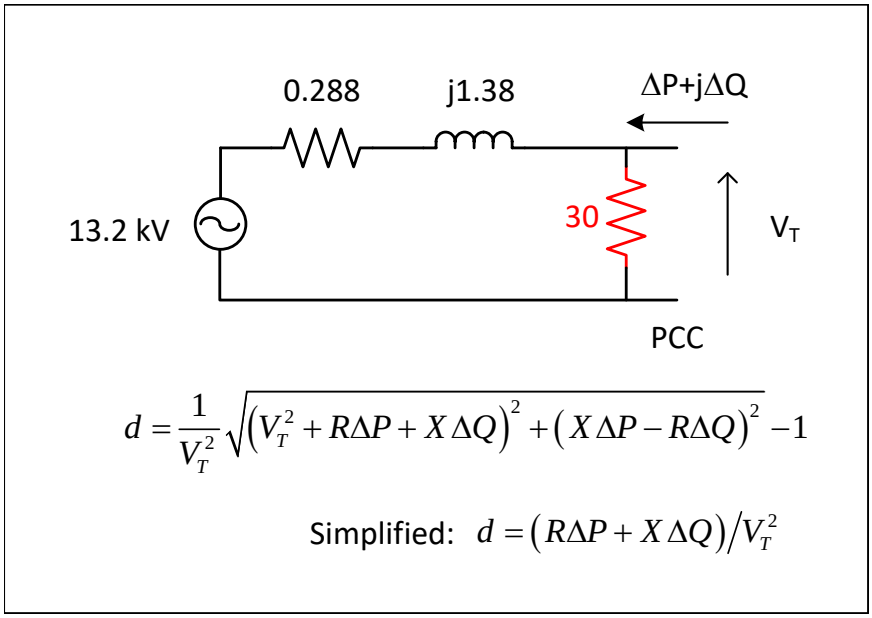

Figure 22. Approximate per-unit voltage change, d, at the point of common coupling.

ratios.

Table 4. The expected voltage change during reactive power step test is about 0.5%

Parameter	Units	No Load +Q	No Load -Q	Full Load +Q	Full Load -Q	Simplified
V_t	kV	13.2	13.2	13.2	13.2	13.2
R	Ω	0.288	0.288	0.347	0.347	0.288
X	Ω	1.380	1.380	1.351	1.351	1.380
ΔP	kW	0	0	0	0	0
ΔQ	kVAR	667.5	-667.5	667.5	-667.5	667.5
d	%	0.529	-0.529	0.518	-0.517	0.529

For the test procedure, it was suggested that only a full-range ΔQ step be performed for minimum and maximum voltage conditions:

1. Feeder voltage dispatched to minimum from DMS, PCC ΔQ = +667.5 kVAR
2. Feeder voltage dispatched to minimum from DMS, PCC ΔQ = -667.5 kVAR
3. Feeder voltage dispatched to maximum from DMS, PCC ΔQ = +667.5 kVAR
4. Feeder voltage dispatched to maximum from DMS, PCC ΔQ = -667.5 kVAR

Steps in ΔP might be considered if the batteries can ramp real power fast enough, i.e., faster than voltage regulator tap changes or other DMS control actions. These tests help validate the model and assumptions for evaluation of smart inverter functions.

4.3 Use Case Test Results

Avista developed a 50-page test plan that incorporated input from PNNL, described above, and from SEL, the microgrid control vendor. The Spirae DER optimization controller was not ready in time for these tests. PNNL observed the first session of off-grid microgrid testing on August 10, 2021, Figure 23. It was necessary for SEL to modify the control code and these tests were completed later in August. The steady state use case tests were also completed successfully, and recorded by Avista. The voltage change at the PCC was about 0.5%, as expected, for changes in Q of 667.5 kVAR.

Figure 23. 500-kW BESS and microgrid control shed behind CCRS, August 10, 2021.

4.4 Building Load Response Tests

After the WA DOC use case testing, WSU Facilities performed building load response tests to help improve the building models, as described in Section 2.0. These were performed from March 3 to March 7, 2022. The buildings have a Niagara automation system that implements two stages of load shedding via thermostat setpoint changes, depicted in Table 5. These were engaged for 60 minutes at approximately 3 p.m. on each test day. The measured response in electrical demand was used to formulate each building's "bid function" for participation in a transactive energy system.

The collected information from the CCRS remote terminal unit (RTU) was:

1. Occupancy (change of value)
2. Room temp (15 min interval)
3. Heating Mode (change of value)

4. Cooling Mode (change of value)

The collected information from the HSB RTU was:

1. Air Handler Mode and status (change of value)
2. Air Handler Fan speed (15 min interval)
3. Air Handler Duct Static (15 min interval)
4. Room controller occupancy/mode (change of value)
5. Room temp (15 min interval)
6. Room Heating/Cooling mode (change of value)
7. Boiler status (change of value)
8. Chiller status (change of value)

We used this information with Avista SCADA data to implement the data-driven models for CCRS and HSB, as discussed in Section 2.0 and [5]. At the CCRS 480V meter, each one-hour load shed produced a reduction of 8 kW out of 20 kW load. At the HSB 480V meter, each one-hour load shed produced a reduction of 25 kW out of 200 kW load. There was no significant change in the 208V loads, because they do not participate significantly in the building HVAC systems, which were the subject of load shedding. The step changes in load resulted from abrupt HVAC shut-off due to thermostat setting changes of several degrees. Because the tests lasted 60 minutes, the building internal temperatures did not change enough to re-engage HVAC system operation. Therefore, the observed reductions may not last beyond 60 minutes.

Table 5. Two load shed stages for CCRS and HSB

Stage	CCRS Setpoint [degF]		HSB Setpoint [degF]	
	Cooling	Heating	Cooling	Heating
Comfort	74	71	74	71
Stage 1 Economy	85	55	78	55
Stage 2 Protect	104	40	104	45

5.0 Conclusions and Recommendations

The main conclusion is that CEF2 SEE met the requirements of all four WA DOC use cases, namely grid services, DER optimization, building fleet optimization, and critical resilience. Simulations and Avista's virtual laboratory helped prepare for the tests, and these tools should be used even more in any future research, development, and deployment (RD&D) projects at Avista. For example, additional testing of microgrid control and DER dispatch software, before field trials, could save time and reduce the risk of errors in the field.

The data-driven approach was successful in representing the CCRS and HSB for transactive energy simulations. Building owners should consider this approach as a simpler and self-calibrating alternative to developing detailed models in EnergyPlus. The required data is available from NOAA for weather, the utility for building electrical meters, and the building automation system. Individual models would improve over time, as more data is collected and incorporated into model training. To encourage more use of this data-driven approach, Avista and WSU may consider whether some of the data could be published:

1. The minimal feeder model from Figure 10.
2. Datasets used to train the CCRS and HSB models.
3. One test case for the consensus-based simulation in TESP.

This building and feeder information would include DER and load sizes, but not other details. PNNL would publish code for the VB agent in Figure 12 in the open-source TESP repository.

The Avista DER and feeder SCADA data has been made available on line to authorized collaborators [14]. This data was helpful in training and validating models, and it could be used in future RD&D projects. For example, many digital meters and relays, e.g., SEL 735 and SEL 451, have the ability to capture transient event data and phasor measurement unit (PMU) data. In some cases, a firmware upgrade is required but not a hardware upgrade. At CEF2 SEE, the recording devices have been connected to Avista's network, which could accommodate the larger volume of PMU and transient data. Uses for this data include:

1. Improving distribution system state estimation with faster sampling rates, higher accuracy, and more precision. PMU data could produce better estimates of phase unbalance, and small phase angle differences, which could improve situational awareness.
2. Transient event data can be used to identify data-driven inverter models for BESS and PV DER. As with buildings, the data and expertise for developing custom inverter models may not be available. Good inverter models are important in dynamic analysis, distribution system protection analysis, and bulk system impacts as DER reaches higher penetration levels.

It is recommended that Avista and its RD&D partners look for more uses of this data from CEF2 SEE. Rather than staging tests, as was done in this project, Avista could set device triggers and automated data transfers to capture events at high sample rates, along with normal operations at slower sample rates.

6.0 References

[1] D. P. Chassin, K. Schneider, and C. Gerkensmeyer. GridLAB-D: An open-source power systems modeling and simulation environment. In *2008 IEEE/PES Transmission and Distribution Conference and Exposition*, pages 1–5, Chicago, IL, USA, April 2008.

[2] James J. Hirsch & Associates. equest: the quick energy simulation tool. https://www.doe2.com/equest/, 10 2003. [Online; accessed 25-July-2022].

[3] U. S. Department of Energy's Building Technologies Office. Energyplus. https://energyplus.net/, 1996. [Online; accessed 25-July-2022].

[4] Pacific Northwest National Laboratory. Transactive Energy Simulation Platform (TESP). https://tesp.readthedocs.io/en/latest/, 2017. [Online; accessed 25-July-2022].

[5] Meghana Ramesh, Jing Xie, Thomas E. McDermott, Monish Mukherjee, Michael Diedesch, and Anjan Bose. Data-driven approaches to transactive energy systems with commercial buildings. in preparation, 2023.

[6] National Oceanic and Atmospheric Administration. Subhourly (5-minute) data from the u.s. climate reference network / u.s. regional climate reference network. https://www.ncei.noaa.gov/pub/data/uscrn/products/subhourly01/, 7 2017. [Online; accessed 12-January-2021].

[7] National Oceanic and Atmospheric Administration. Integrated surface dataset (global). https://www.ncei.noaa.gov/access/search/data-search/global-hourly. [Online; accessed 12-January-2021].

[8] Monish Mukherjee, Erik Lee, Anjan Bose, John Gibson, and Thomas E. McDermott. A cim based data integration framework for distribution utilities. In *2020 IEEE Power & Energy Society General Meeting (PESGM)*, pages 1–5, 2020.

[9] Roger C. Dugan and Thomas E. McDermott. An open source platform for collaborating on smart grid research. In *2011 IEEE Power and Energy Society General Meeting*, pages 1–7, Detroit, MI, USA, July 2011.

[10] J. C. Fuller, K. P. Schneider, and D. Chassin. Analysis of residential demand response and double-auction markets. In *2011 IEEE Power and Energy Society General Meeting*, pages 1–7, 2011.

[11] Donald J. Hammerstrom and Hung Ngo. A transactive network template for decentralized coordination of electricity provision and value. In *2019 IEEE PES Transactive Energy Systems Conference (TESC)*, pages 1–5, 2019.

[12] Peng Wang, Bishnu Bhattarai, Jianming Lian, Donald J. Hammerstrom, and Ke Ma. A unified virtual battery model for responsive assets. In *2019 IEEE Power & Energy Society General Meeting (PESGM)*, pages 1–5, 2019.

[13] D Wu, S Huang, K Oikonomou, R Hu, B Huang, CK Vartanian, X Xa, A Crawford, and M Diedesch. Avista's shared energy economy model pilot: A techno-economic assessment. Technical Report PNNL SA-00000, Pacific Northwest National Laboratory, 7 2022.

[14] Avista Corporation. Avista digital exchange. https://energy.collaboratives.io/login, 2 2022. [Online; accessed 17-February-2022].

Pacific Northwest National Laboratory

902 Battelle Boulevard
P.O. Box 999
Richland, WA 99354
1-888-375-PNNL (7675)

www.pnnl.gov